Energy Conversion and Management 50 (2009) 1506–1512

Contents lists available at ScienceDirect

Energy Conversion and Management

journal homepage: www.elsevier.com/locate/enconman

Thermoelectric automotive waste heat energy recovery using maximum power point tracking

Chuang Yu *, K.T. Chau

Department of Electrical and Electronic Engineering, The University of Hong Kong, Pokfulam Road, Hong Kong

ARTICLE INFO

Article history:
Received 21 May 2008
Received in revised form 18 January 2009
Accepted 27 February 2009
Available online 1 April 2009

Keywords:
Automotive
Energy recovery
Maximum power point tracking
Thermoelectric generator
Waste heat

ABSTRACT

This paper proposes and implements a thermoelectric waste heat energy recovery system for internal combustion engine automobiles, including gasoline vehicles and hybrid electric vehicles. The key is to directly convert the heat energy from automotive waste heat to electrical energy using a thermoelectric generator, which is then regulated by a DC–DC Ćuk converter to charge a battery using maximum power point tracking. Hence, the electrical power stored in the battery can be maximized. Both analysis and experimental results demonstrate that the proposed system can work well under different working conditions, and is promising for automotive industry.

1. Introduction

With ever increasing price of oil and growing concern on energy conservation, the development of energy-efficient technologies for automobiles has taken on an accelerated pace. Electric vehicles used to be considered as the most energy-efficient and environmental road transportation [1]. However, the available energy sources for electric vehicles are of insufficient capacity to enable them directly competing with existing gasoline automobiles [2]. In recent years, hybrid electric vehicles have been identified as the most feasible energy-efficient road transportation, although they are not of absolutely zero emission [3]. Nevertheless, both gasoline vehicles and hybrid electric vehicles have employed internal combustion engines which are inefficient. Fig. 1 shows a typical energy flow path of an internal combustion engine in which only about 25% of the fuel combustion can be utilized for vehicle operation, whereas about 40% is lost in the form of waste heat of exhaust gas [4]. As a result, the average temperature of the exhaust manifold is over 250 °C.

In parallel with the improvement of the efficiency of internal combustion engines, many researchers actively investigate the use of thermoelectric (TE) technology to recover the waste heat energy for gasoline vehicles [5–7], and hybrid electric vehicles [8,9]. The corresponding research activities have been focused on the development of TE materials which can offer higher energy conversion efficiency and wider operating temperature range of internal combustion engines [5,7]. Recently, the investigation has been extended to the development of the whole TE waste heat energy recovery system. However, such investigation is mainly under feasibility study [6,9].

The maximum power point tracking (MPPT) is a well-known control technique which can enable the photovoltaic (PV) power system to operate at its maximum power capability under various sunlight intensities [10]. Very recently, this control technique has been introduced into the thermoelectric generation (TEG) power system [11,12]. In [11], the corresponding MPPT technique is based on the battery current feedback only, while assuming the battery voltage to be constant. However, all practical batteries have a significant change of terminal voltages, especially during charging, which should not be neglected. In [12], the corresponding MPPT technique is based on the measurement of power which is derived from the TEG terminal voltage and current. However, such maximization has not taken into account the power converter loss, which should not be a constant.

In this paper, a new TE waste heat energy recovery system is proposed and implemented for internal combustion engine automobiles. Instead of using the TEG terminal voltage and current, the MPPT controller will utilize the battery terminal voltage and current to maximize the output power, thus taking into account the battery voltage variation and the non-constant power converter loss. Also, the DC–DC Ćuk converter will be used to regulate the power flow between the TEG and the battery pack. It takes the definite advantages that both of its input current and output current are non-pulsating, which can significantly minimize the

* Corresponding author.
E-mail address: chuangyu@eee.hku.hk (C. Yu).

0196-8904/$ - see front matter © 2009 Elsevier Ltd. All rights reserved.
doi:10.1016/j.enconman.2009.02.015

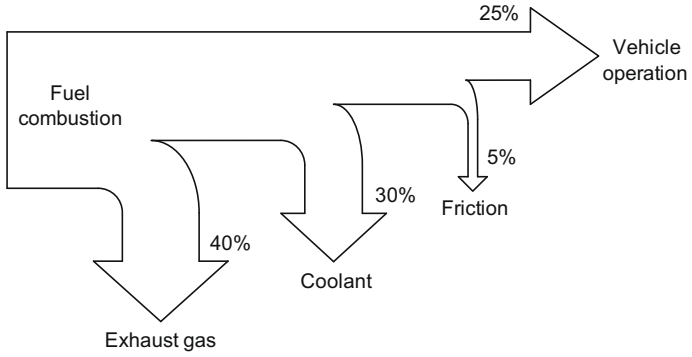

Fig. 1. Energy flow path in internal combustion engine.

disturbance on TEG operation and enhance the battery current measurement.

In Section 2, the TEG will be introduced, and its characteristics will be described. In Section 3, the waste heat energy recovery system for internal combustion engine automobiles will be discussed. Then, Section 4 will be devoted to presenting the proposed power conditioning system, including the Ćuk converter and the MPPT controller. In Section 5, experimental results will be given to verify the validity of the proposed system. Finally, Section 6 will discuss the uncertainties and equipment errors in the experiment and their impacts on the results.

2. Thermoelectric generation

The Seebeck effect is the conversion of temperature differences directly into electricity. This effect was first discovered by Thomas Johann Seebeck in 1821, who found that a voltage existed between two ends of a metal bar when a temperature gradient existed in the bar. Based on the Seebeck effect, the TEG system takes the advantages of no moving parts, silent operation and very reliable. For automobiles, including both gasoline vehicles and hybrid electric vehicles, the waste exhaust heat can be recovered directly to electrical energy for battery charging, thereby increasing the overall vehicle fuel efficiency.

Fig. 2 depicts a single TEG couple in which the n-type and p-type semiconductor materials are configured thermally in parallel and electrically in series. As the heat moves from hot sides to cold sides, the accumulation of charge carriers in semiconductors generates an electrical potential between the ends of this TEG couple. Typically, in a practical TEG device, about 120 such TEG couples are connected in series to bring the voltage up to a useful level. In this paper, an experimental TEG system is shown in Fig. 3 in which six TEG devices are connected in series, and then sandwiched tightly between a copper radiator and a copper plate. The water-cooled copper radiator serves as the cold sides of all TEG devices, while the copper plate works as the hot sides of all the devices.

A single Bi–Te based TEG device is used for exemplification. An electric heater is used to provide different hot-side temperatures: 100, 150, 200 and 250 °C, while the cold-side temperature is maintained at 50 °C by using a water-cooled radiator. The corresponding open-circuit output voltages are measured as 2.02, 3.52, 4.56 and 5.25 V, respectively. Then, by varying the load resistance from 2 to 10 Ω, the output voltage, output current and output power of the device versus the load resistance R_l under different hot-side temperatures are recorded as shown in Figs. 4–6, respectively. Consequently, after connecting six TEG devices in series, the open-circuit voltage V_g and the corresponding internal resistance R_g of the whole TEG system under different hot-side temperatures are obtained as shown in Fig. 7. It can be observed that both V_g and R_g increase with the temperature difference ΔT. In order to enable the maximum power transfer from the source to the load, R_g needs to be equal to R_l. Thus, the maximum power transfer can be achieved when R_l is controlled in accordance with ΔT.

3. Automotive waste heat energy recovery

Basically, a practical automotive waste heat energy recovery system consists of an exhaust gas system, a heat exchanger, a TEG system, a power conditioning system, and a battery pack. There are various considerations and alternatives:

- A typical exhaust gas system for internal combustion engines is composed of the exhaust manifold, exhaust pipe, catalytic converter, center muffler and rear muffler. It is a natural choice that the heat exchanger should be installed at the location with the highest temperature, namely at the exhaust manifold. Taking into account the working temperature of the TEG device and the convenience of mounting the heat exchanger, a compromise may be required on the selection of heat exchanger location.

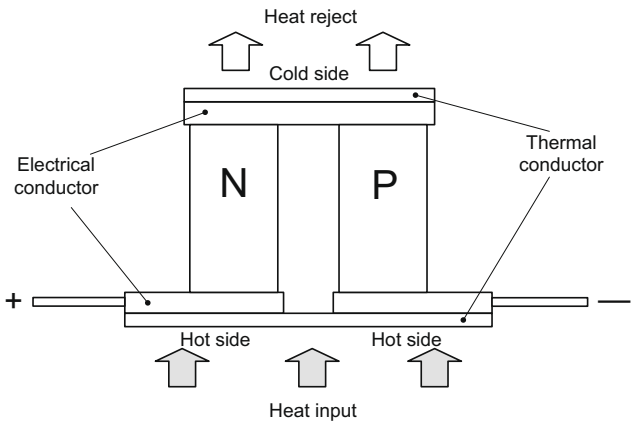

Fig. 2. Configuration of TEG couple.

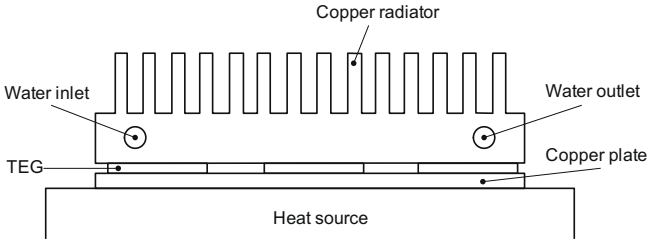

Fig. 3. Configuration of experimental TEG system.

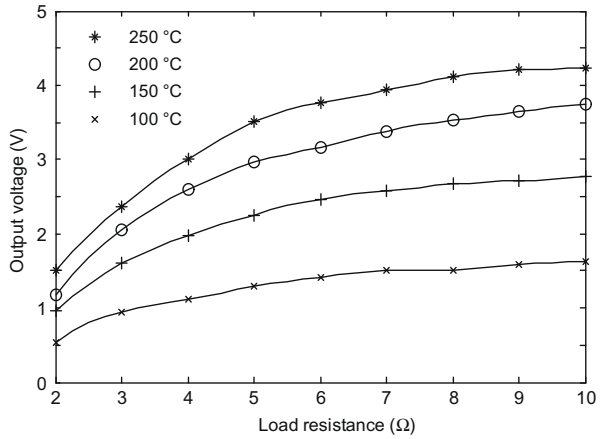

Fig. 4. Output voltage characteristics of TEG device.

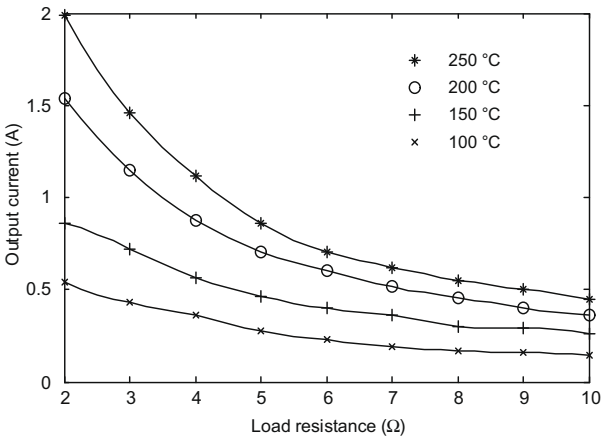

Fig. 5. Output current characteristics of TEG device.

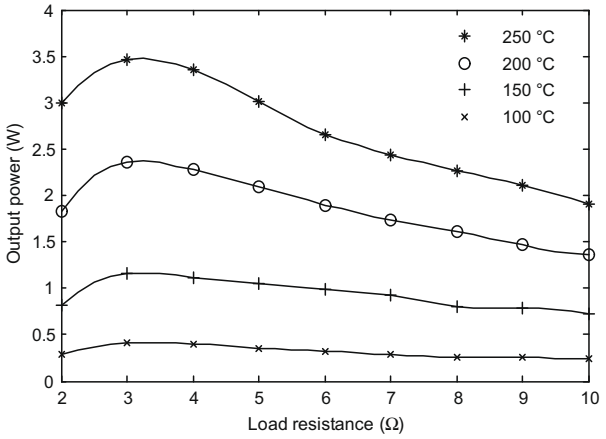

Fig. 6. Output power characteristics of TEG device.

- The heat exchanger can directly combine with the TEG system to form a united system, hence offering a compact structure. Alternatively, the heat exchanger can work with the TEG system by means of a pump which circulates the working fluid between them. The use of this pumping loop allows for a wider variation of exhaust gas flow and hence thermal flux. It should be noted that the design of heat exchanger involves a tradeoff between the thermal exchanger efficiency and the exhaust gas flow rate.

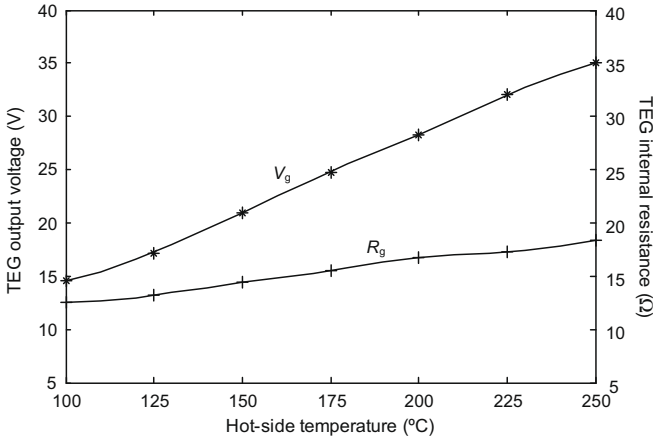

Fig. 7. Output voltage and internal resistance characteristics of TEG system.

- The TEG system is governed by the selected TE materials which need to offer high energy conversion efficiency, namely the figure of merit ZT as defined by $ZT = S^2T/\kappa\rho$ where S is the thermoelectric power, T is the absolute temperature, κ is the total thermal conductivity and ρ is the electrical resistance [6]. In recent years, the characteristics of thermoelectric materials have been significantly improved in terms of both the ZT value and the temperature range. For example, the p-type and n-type Bi–Te materials offer the optimal ZT values at the temperature range of exhaust gas.
- Rather than directly connecting the TEG system to the battery pack, a power conditioning system needs to be installed between them as shown in Fig. 8. This power conditioning system functions to regulate the power flow in such a way that the maximum power transfer can be achieved. The two key issues are the design of a proper power converter and the devise of an effective control algorithm, which will be discussed later.

Consequently, the proposed TE waste heat energy recovery system for automobiles is shown in Fig. 9. Firstly, when the internal combustion engine operates, the heat exchanger mounted on the catalytic converter of the exhaust gas system captures the waste heat. Secondly, the thermal energy of the heat exchanger is transferred to the TEG system, which directly generates electricity. Finally, the power converter performs power conditioning in such a way that the maximum power transfer can be attained.

4. Proposed power conditioning

4.1. Ćuk converter

Since its invention in 1977 [13], the Ćuk converter has received much attention from the arena of power electronics. Its major asset is that both input and output currents are continuous, namely

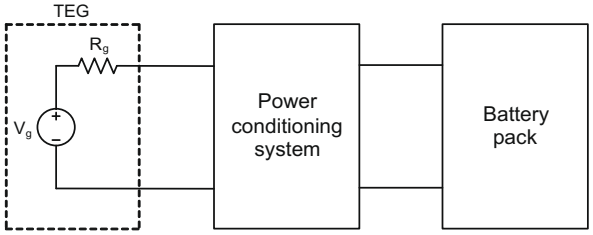

Fig. 8. TEG power system.

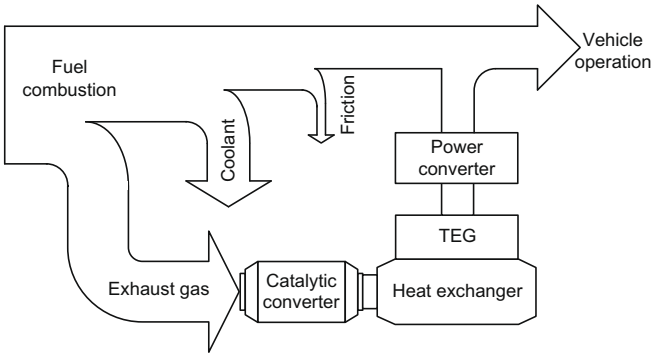

Fig. 9. Waste heat energy recovery system.

there is no time gap where the ripple current falls to zero. By winding the input and output inductors on the same core, the ripple amplitude can be reduced to zero. This feature is utmost important for the proposed power conditioning; otherwise, a pulsating input current will greatly disturb the operating point of the TEG device, while a pulsating output current will significantly perturb the battery voltage level.

A basic Ćuk converter is shown in Fig. 10. When the switching frequency f_s is sufficiently high or the capacitance C_1 is sufficiently large, the converter always operates with a continuous capacitor voltage, so-called the continuous capacitor voltage (CCV) mode. In this mode of operation, there are two topological stages as shown in Fig. 11, in which the switch S is turned on within the period of δT_s and turned off within the period of $(1-\delta)T_s$, where δ is the duty cycle and T_s is the switching period. The corresponding theoretical waveforms are shown in Fig. 12.

From its principle of operation, the voltage conversion gain, namely the ratio of output voltage V_o to input voltage V_i can be easily deduced as:

$$\frac{V_o}{V_i} = -\frac{\delta}{1-\delta} \tag{1}$$

which indicates that V_o can be larger or smaller than V_i, depending on the value of δ, while the minus sign denotes that the terminals of V_o and V_i are of opposite polarity. Taking the average currents flowing through the inductors L_1 and L_2 be I_1 and I_2, respectively, the capacitor voltage V_c and the diode voltage V_d can be expressed as:

$$V_c = \begin{cases} V_2 + \frac{I_2}{C_1}(-t+\delta T_s) & 0 < t < \delta T_s \\ V_2 + \frac{I_1}{C_1}(t-\delta T_s) & \delta T_s < t < T_s \end{cases} \tag{2}$$

$$V_d = \begin{cases} V_c & 0 < t < \delta T_s \\ 0 & \delta T_s < t < T_s \end{cases} \tag{3}$$

where V_2 is the minimum value of V_c. At steady state, the average voltage across L_1 and L_2 are both zero. Hence, V_i is equal to the average value of $(V_c - V_d)$, which can be deduced as:

$$V_i = \frac{1}{T_s}\int_0^{T_s}(V_c - V_d)dt = V_2(1-\delta) + \frac{I_1 T_s}{2C_1}(1-\delta)^2 \tag{4}$$

Hence, the input resistance of the converter can be obtained as:

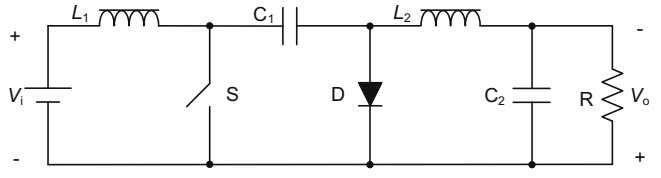

Fig. 10. Basic Ćuk converter.

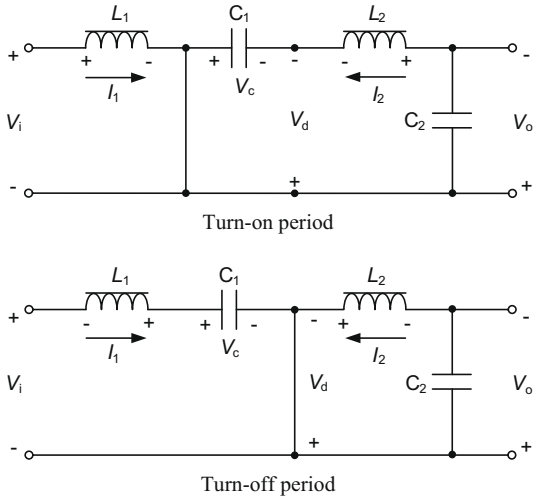

Fig. 11. Topological stages in CCV mode.

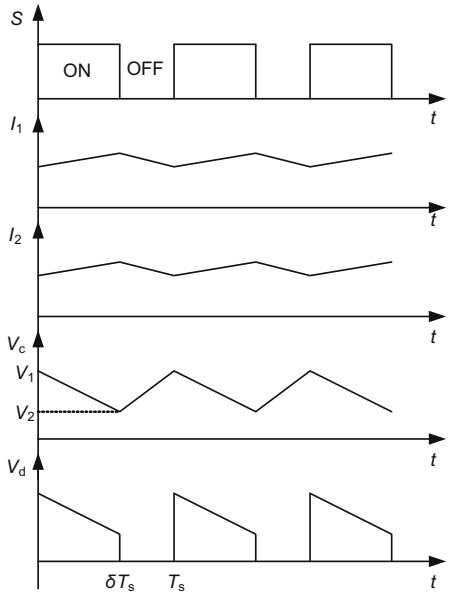

Fig. 12. Theoretical waveforms in CCV mode.

$$R_i = \frac{V_i}{I_1} = \frac{V_2(1-\delta)}{I_1} + \frac{(1-\delta)^2}{2f_s C_1} \tag{5}$$

It can be found that R_i changes with δ, namely R_i increases with the decrease of δ and vice versa for $\delta \in [0,1]$.

4.2. MPPT control

MPPT control has been widely implemented in PV power systems, and its effectiveness is well proven. There are many MPPT control techniques that have been proposed. Among them, the perturb-and-observe (P&O) technique, incremental-conductance technique, parasitic-capacitance technique and constant-voltage technique are considered to be viable for practical implementation [10].

The P&O technique is an iterative approach that perturbs the operating point of the PV power system and then observes the output power so as to determine the direction of change for maximizing the output power. Thus, the maximum power can be eventually

achieved by forcing the derivative of output power to be equal to zero under power feedback control. It takes the definite advantages that there is no need to have an accurate model of the PV power system, and the online searching process can automatically handle minor parameter variations. However, this MPPT technique is unsuitable for those PV power systems under rapidly changing atmospheric condition.

As the TEG power system has similar voltage–current (V–I) characteristics as the PV power system, it can borrow the MPPT techniques that have been developed for the PV power system. Since the operating temperature of the internal combustion engine does not have a rapid change, the aforementioned shortcoming of the P&O technique will not occur at the TEG power system. So, this MPPT technique is adopted for the proposed waste heat energy recovery system.

4.3. Implementation

The proposed power conditioning system is implemented as shown in Fig. 13. It consists of the TEG system, the Ćuk converter, the MPPT controller and the battery pack. The TEG system is configured by connecting six Bi–Te TEG devices in series. The MPPT controller is digitally implemented by a low-cost microcontroller which possesses an analog-to-digital converter (ADC) to capture the feedback signals and a direct pulse-width-modulated (PWM) output to drive the power MOSFET of the Ćuk converter.

As illustrated in Fig. 8, the maximum power transfer occurs when R_g of the TEG system equals R_i of the Ćuk converter. Meanwhile, (5) shows that R_i is a function of δ. Therefore, by tuning δ properly, R_i can match with R_g, hence achieving maximum power transfer at different temperatures. Compared with the previous works, this power conditioning system offers two important features:

- Both the battery voltage and battery current are online measured and used to calculate the output power. Thus, the variation of battery voltage during charging can be taken into account. It should be noted that this voltage variation may be over 20% for the commonly used lead–acid battery [1].
- Rather than maximizing the TEG output power, the MPPT controller maximizes the converter output power which is the actual power that can be stored in the battery. It should be noted that the maximum battery power may not be coincident with the maximum TEG output power, since the converter power loss may not be constant. So, the use of load power for MPPT can virtually maximize the power output of the whole power conditioning system.

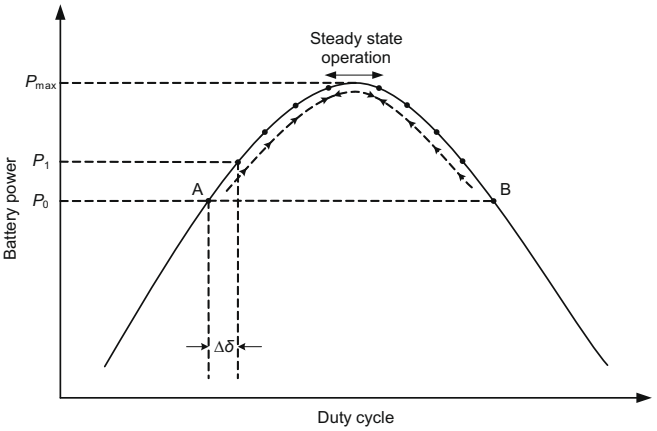

Fig. 14. Searching process of MPPT control.

The implementation of the P&O technique for MPPT is shown in Fig. 14. Initially, the proposed power conditioning system works with a duty cycle δ_0 at the operating point A or B. The corresponding output power is denoted as P_0. In the first perturbation, a positive increment of duty cycle $\Delta\delta$ is applied so that a new output power P_1 is resulted. By comparing with the previous value, if P_1 not less than P_0 is observed, it means that the starting point is A, and δ will keep on increasing in the next iteration until the maximum output power P_{max} is reached. In contrast, if P_1 less than P_0 is observed, it indicates that the starting point is B, and δ will be reduced by changing the sign of $\Delta\delta$ so as to achieve a higher power in the next iteration. By repeating this searching process, namely maintaining the direction if the new power is not less than the previous power, whereas reversing the direction if the new one is less than the previous one, the system will eventually operate at around P_{max}. The corresponding program flowchart is also shown in Fig. 15.

5. Experimental results

In order to enable a manageable environment for experimentation, the proposed waste heat energy recovery system is simplified in such a way that the TEG power system adopts only six TEG devices connected in series, the heat exchanger is emulated by an electric heater, and the load is a 6 V lead–acid battery pack. Throughout the experimentation, the hot-side and cold-side temperatures of the TEG system are measured by using K-type thermocouples, while the cold-side temperature is always kept at around

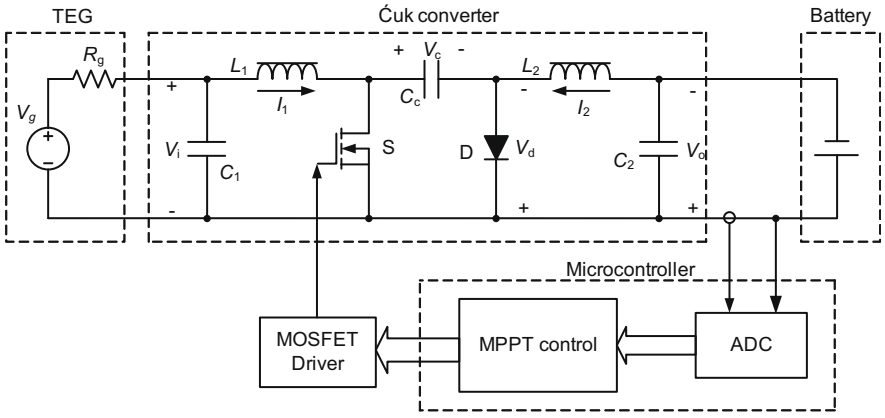

Fig. 13. System implementation.

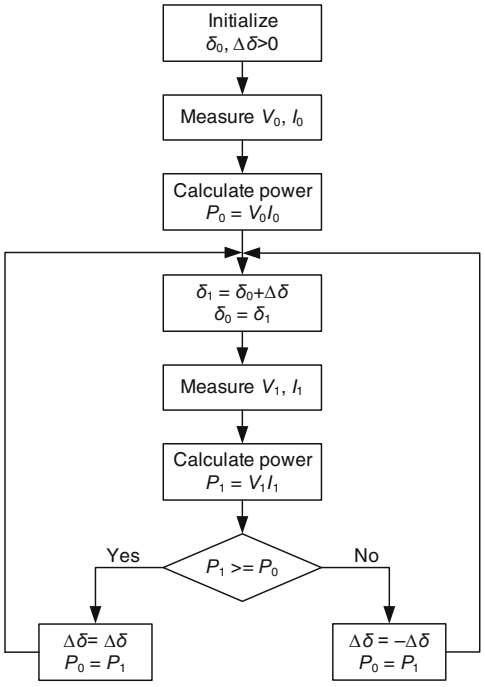

Fig. 15. Program flowchart of MPPT control.

50 °C. The switching frequency of the Ćuk converter is also kept constant at 21.6 kHz.

To assess whether the MPPT controller works properly, the initial duty cycle is set to 20% and then to 90% for each hot-side temperature, namely 100, 125, 150, 175, 200, 225 and 250 °C. It can be found that the system can quickly settle at the same maximum load power or maximum battery power for both $\delta_0 = 20\%$ and $\delta_0 = 90\%$ with $\Delta\delta = 1\%$. It confirms that the system can perform MPPT under arbitrary initial duty cycle at different temperatures. The corresponding battery power characteristics are shown in Fig. 16. These characteristics also reveals that when the hot-side temperature increases from 100 to 250 °C, the duty cycle for MPPT decreases from 65% to 50%. It fully agrees with our expectation: the higher the hot-side temperature, the higher the value of R_g, the higher the value of R_i is desired, hence the smaller the value of δ is adopted for MPPT.

Moreover, the battery voltage and currents at the hot-side temperature of 200 °C are measured as shown in Fig. 17. It can be found that the battery voltage varies between 6 and 7.3 V, thus exhibiting a variation of 21.6%. Hence, it confirms that this battery voltage should not be assumed constant.

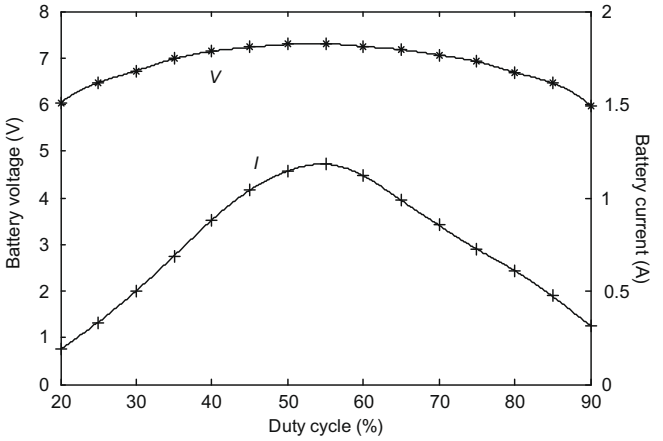

Fig. 17. Battery voltage and current versus duty cycle at 200 °C.

Finally, the effectiveness of the proposed MPPT is evaluated by comparing the experimental results with those obtained by using a fixed duty-cycle Ćuk converter and using direct connection. The fixed duty cycle is set at 50%, which is almost the optimal value at 250 °C. The corresponding maximum battery power at different hot-side temperatures are shown in Fig. 18, where P_{opt}, P_{fix} and P_{dir} referred to the maximum power obtained by using the optimal duty-cycle Ćuk converter with MPPT control, the fixed duty-cycle Ćuk converter without MPPT control, and the direct connection without Ćuk converter, respectively. As expected, the proposed power conditioning system exhibits improvement over the others. In order to quantify the improvement, the following two indicators are defined:

$$\Delta P_1 = \frac{P_{opt} - P_{fix}}{P_{fix}} \times 100\% \quad (6)$$

$$\Delta P_2 = \frac{P_{opt} - P_{dir}}{P_{dir}} \times 100\% \quad (7)$$

So, the corresponding percentages in power improvement are also plotted with dashed lines in Fig. 18. It can be seen that the power improvements are significant, up to $\Delta P_1 = 14.5\%$ and $\Delta P_2 = 22.6\%$ at the temperature of 100 °C. These improvements agree with the expectation, since the converter operating at a fixed duty cycle

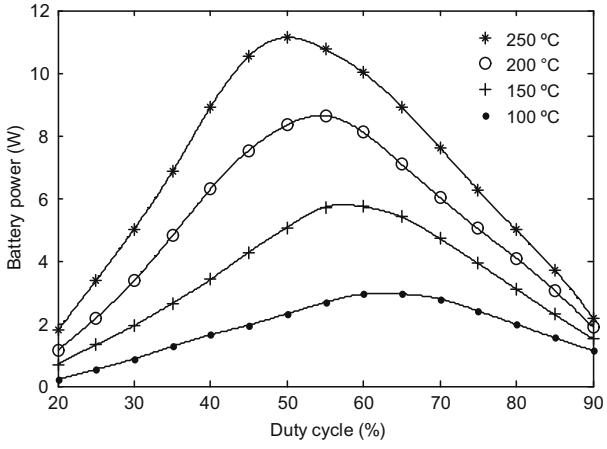

Fig. 16. Battery power versus duty cycle at different temperatures.

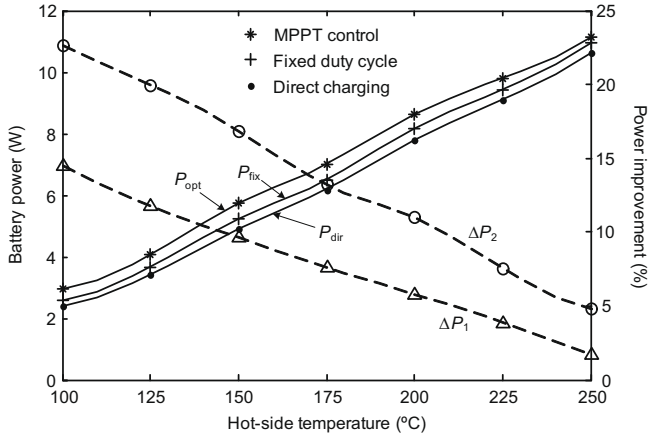

Fig. 18. Maximum battery power and power improvement at different temperatures.

Table 1
Accuracy of measurements.

Measurement	Equipment	Accuracy
Voltage V	Power analyzer PA2200	±0.1% (reading) ±0.1% (range) ±0.01% per kHz ±10 mV
Current I		±0.1% (reading) ±0.1% (range) ±0.02% per kHz ±2 mA
Power P		±0.2% (reading) ±0.1% (range) ±2mW ±(0.02/PF)% per kHz
Temperature T	Thermometer with K-type thermocouple UT327	±0.85% (reading) ±0.7 °C

Table 2
Impacts of measurement accuracy on power improvement.

	100 °C	125 °C	150 °C	175 °C	200 °C	225 °C	250 °C
ΔP_1 (%)	14.51	11.77	9.613	7.614	5.788	3.869	1.648
$\Delta P'_1$ (%)	10.46	8.942	7.646	6.045	4.548	2.805	0.741
ΔP_2 (%)	22.61	19.95	16.86	13.18	10.96	7.540	4.817
$\Delta P'_2$ (%)	18.12	16.79	14.69	11.49	9.630	6.419	3.867

cannot perform effective power transfer when the operating temperature deviates from its predefined optimal temperature (δ = 50% for 250 °C).

It should be noted that a practical TEG system may connect over 120 TEG devices in series, (over 20 times of the current experimental system), and the working temperature at the exhaust manifold may over 750 °C (over 3 times of the current experimental system), the recovered power can be over 600 W which accounts for about 50% power consumption of automotive electronics. Therefore, the proposed waste heat energy recovery system is essential for all internal combustion engine vehicles.

6. Discussion

There are four major variables that need measurements in the experiment, namely the battery voltage, battery current, battery power and operating temperature. The voltage, current and power are online measured by a power analyzer (AV Power PA2200), while the temperature is online recorded by a digital thermometer equipped with K-type thermocouple (UNI-T UT327). The corresponding accuracy of measurements is listed in Table 1.

Throughout the experiment, the selected voltage range and current range are 14 V and 1.8 A, respectively. Since both the voltage and current are DC, the effects of frequency and power factor (PF) are absent in the power measurement. For example, when the maximum power at 250 °C is measured as 11.133 W, the accuracy of power measurement can readily be calculated by using the tabulated accuracy in Table 1, namely $\pm E_{P\max} = \pm 49.5$ mW. Taking into account the maximum error in power measurement, the worst scenarios of power improvement can be deduced from (6) and (7) as given by:

$$\Delta P'_1 = \frac{(P_{opt} - E_{P\max}) - (P_{fix} + E_{P\max})}{P_{fix} + E_{P\max}} \times 100\% \quad (8)$$

$$\Delta P'_2 = \frac{(P_{opt} - E_{P\max}) - (P_{dir} + E_{P\max})}{P_{dir} + E_{P\max}} \times 100\% \quad (9)$$

Hence, the originally measured power improvement ΔP_1 and ΔP_2 are compared with the worst-scenario power improvement $\Delta P'_1$ and $\Delta P'_2$ at different temperatures as listed in Table 2. It can be seen that even under the worst-scenario accuracy of measurements, the power obtained by using the proposed MPPT method can still provide significant improvement over the other two methods.

Concerning the accuracy of temperature measurement, the reading error can be easily calculated by using the tabulated accuracy in Table 1. Namely, the maximum reading error occurs at 250 °C and is given by $\pm E_{T\max} = \pm 2.825$°C, while the minimum reading error at 50 °C is $\pm E_{T\min} = \pm 1.125$°C. As depicted in Table 2, this temperature reading error does not significantly affect the percentage of power improvement.

7. Conclusions

In this paper, an automotive TE waste heat energy recovery system has been proposed and implemented. The proposed system has newly adopted the Ćuk converter for power conditioning, since it can offer non-pulsating input and output currents which can minimize the disturbance to the TEG and the battery, respectively. Also, the MPPT control has newly utilized both the battery voltage and battery current to maximize the power transfer, since it can take into account the variation of battery voltage during charging and the non-constant power loss in the converter. After prototyping the whole system, the experimental results confirm that the MPPT can be successfully performed at arbitrary initial duty cycles, and the resulting power improvements can be up to 14.5% and 22.6% compared with the cases without using MPPT and even without power conditioning, respectively. The accuracy of measurements and its impact on power improvement have also been discussed.

Acknowledgment

This work is funded by a grant (Project No. 200807176032) from the Committee on Research and Conference Grants, The University of Hong Kong, China.

References

[1] Chau KT, Wong YS, Chan CC. An overview of energy sources for electric vehicles. Energy Convers Manage 1999;40(10):1021–39.
[2] Chau KT, Wong YS. Hybridization of energy sources in electric vehicles. Energy Convers Manage 2001;42(9):1059–69.
[3] Chau KT, Wong YS. Overview of power management in hybrid electric vehicles. Energy Convers Manage 2002;43(15):1953–68.
[4] Stabler F. Automotive applications of high efficiency thermoelectrics. DARPA/ONR/DOE high efficiency thermoelectric workshop; 2002. p. 1–26.
[5] Matsubara K. Development of a high efficient thermoelectric stack for a waste exhaust heat recovery of vehicles. In: International conference on thermoelectrics; 2002. p. 418–23.
[6] Yang J. Potential applications of thermoelectric waste heat recovery in the automotive industry. In: International conference on thermoelectrics; 2005. p. 155–9.
[7] LaGrandeur J, Crane D, Hung S, Mazar B, Eder A. Automotive waste heat conversion to electric power using skutterudite, TAGS, PbTe and BiTe. In: International conference on thermoelectrics; 2006. p. 343–48.
[8] Chau KT, Chan CC. Emerging energy-efficient technologies for hybrid electric vehicles. Proc IEEE 2007;95(4):821–35.
[9] Smith K, Thornton M. Feasibility of thermoelectrics for waste heat recovery in hybrid vehicles. Paper no. 266. In: International electric vehicle symposium and exposition; 2007.
[10] Hohm DP, Popp ME. Comparative study of maximum power tracking algorithms. Prog Photovolt: Res Appl 2003:47–62.
[11] Eakburanawat J, Boonyaroonate I. Development of a thermoelectric battery-charger with microcontroller-based maximum power point tracking technique. Appl Energy 2006;83(7):687–704.
[12] Yu C, Chau KT, Chan CC. Thermoelectric waste heat energy recovery for hybrid electric vehicles. Paper no. 21. In: International electric vehicle symposium and exposition; 2007.
[13] Ćuk S, Middlebrook RD. A new optimum topology switching dc-to-dc converter. In: IEEE power electronics specialists conference; 1977. p. 1–20.